

Optical Properties of Two-Dimensional Dielectric Perforated Waveguide with Variable Hole-Type Defect

K.M. GRUSZKA* AND M. DOŚPIAŁ

^aDepartment of Physics, Czestochowa University of Technology,
al. Armii Krajowej 19, 42-200 Czestochowa, Poland

Doi: [10.12693/APhysPolA.142.101](https://doi.org/10.12693/APhysPolA.142.101)

*e-mail: konrad.gruszka@pcz.pl

In this paper, we present the results of systematic studies on optical wave propagation thru a dielectric, perforated waveguide with a variable radius of hole-type defect. Such structures represent photonic crystals-like behaviour due to a finite number of periodic perforations, and their properties are strongly dependent on the geometrical shape of the central irregularity. By changing the radius of this defect, we can show that the resonant mode is trapped and localized at the defect position, while if there is continuity preserved in the perforations, no resonant mode is observed. All calculations were made using finite difference time-domain method.

topics: finite difference time-domain method (FDTD), waveguide, defect, EM propagation

1. Introduction

Photonic waveguides are the subject of many recent studies [1–4] because of scientists's interest in various photonic devices that apply the useful waveguide properties to transmit electromagnetic waves. At the same time, also a second big family of photonic devices, known as photonic crystals, is of unflagging interest, due to the presence of a forbidden photonic gap in these materials related to their geometrical structure [5–7]. The presence of this forbidden gap is especially desirable as the band gap engineering allows the fine tuning of the material properties to a specific application [8–10]. For this reason, wanting to combine both families of optical materials, we present here the results of numerical studies of a modified waveguide, which is constructed by combining the periodicity of a photonic crystal (meta-atoms) with a typical waveguide. As a result, we hope to obtain a hybrid structure that should have combined properties. Such an approach will make it possible to study the effect of placing a structure defect in the form of periodicity disturbance.

Obviously, taking into account the finite size of the waveguide, it is impossible to realize a typical ideal photonic crystal on it, which requires the application of periodic boundary conditions in at least one dimension of space. Therefore, our approach to this problem is different and we will only place a finite number of meta-atoms (in this case holes) in the waveguide structure, similarly to the approach in [11]. The authors studied there the resonant scattering and wave propagation across waveguide,

showing the emergence of resonant frequencies at which the wave was almost fully transmitted. There are also different approaches to construct a waveguide using embedded periodic structure. For example, in [12] and [13], the waveguide structure is based on photonic crystal and the transmitting channel is made by removing periodic elements. This technique is also successfully used for mechanical (sound) waves with similar results to the electromagnetic case, however, the structures obtained are usually much larger in size [14]. Such similar structures for electromagnetic waves can be successfully created experimentally, as for example, shown by Hubner et al. [15, 16]. Namely, these authors show some aspects of the fabrication of photonic crystal (PC) structures in a polymer waveguide material on different waveguide substrate materials [15], and in [16] they use the femtosecond laser to micro-machine one-dimensional photonic crystal channel waveguides.

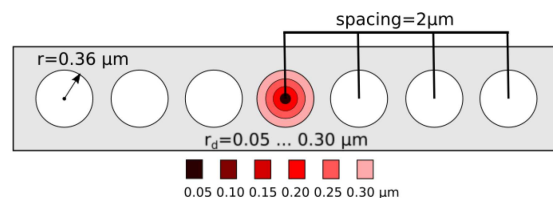


Fig. 1. Schematic diagram of waveguide with variable hole-defects. The spacing between the hole centers is always fixed to $2 \mu\text{m}$ on both sides of the defect. For ease of readability, we present only selected defect sizes.

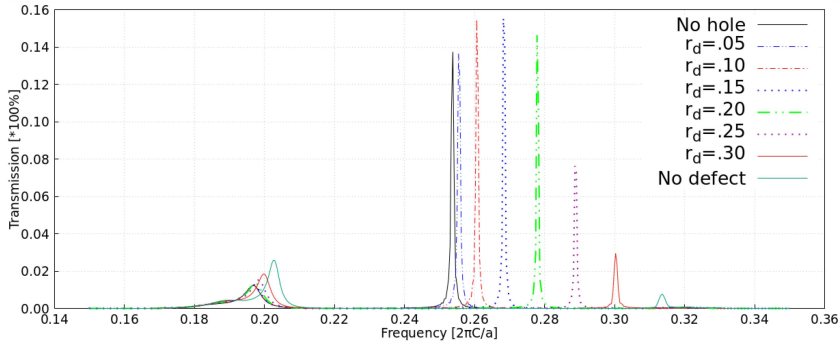


Fig. 2. Transmission spectrum for different size (radius) of defects ranging from 0.05 up to 0.3 μm . Between resonant mode peaks a bandgap is clearly seen for each of studied defects.

In this paper, we present the results of the finite difference time-domain method (FDTD) calculation for a modified finite waveguide with a variable defect diameter ranging from 0.05 to 0.30 and with a cavity between the meta-atoms that is without defect.

2. Computational methods

For the whole calculations, we have used the MEEP software package [17], which implements the finite difference time-domain (FDTD) method to simulate electromagnetism. The schematic structure of the waveguide is presented in Fig. 1. We choose silicon with the dielectric constant $\epsilon_w = 11.8$ as the waveguide material. The three regular holes placed on each side of the defect are filled with air ($\epsilon_a = 1$) and their radius is set to 0.36 μm . Also, the whole waveguide is immersed in the air. Then, we placed a Gaussian pulse source in such constructed waveguide to explore the frequency response of defected and pristine waveguide. The horizontal length of such a waveguide is 13 μm while its thickness is set to 1.2 μm . To obtain a band diagram of an infinite ideal photonic crystal waveguide (without defects), we constructed a small cell with Bloch periodic boundary conditions in one dimension (along the k_x vector) and placed selectively perfectly matched layers (PML's) only in the y direction with a thickness of 1 μm , due to the symmetry of irreducible Brillouin zone. For transmission studies, we have used PML as scattered wave absorbent surrounding the entire simulation domain with the thickness set to 1 μm . In both cases, we carefully tested the required PML thickness to minimize wave scattering.

3. Results and discussion

In Fig. 2, the transmission spectrum for different defect radii r_d ranging from 0.05 to 0.3 μm is shown. Additionally, we also present the waveguide configuration without defect in which the continuity of the meta-atoms is preserved (marked as no defect) and with no hole — corresponding to the situation

when there is a gap instead of a hole between adjacent 3-meta-atom groups maintaining the gap size. In the “no hole” case, there is a cavity between adjacent 3-holes, which is seen to be a trap for the resonant mode located at 0.255 $[2\pi C/a]$. Further introduction of a finite size defect, as can be clearly seen, introduces for each defected system an additional third peak visible for example for $r_d = 0.20 \mu\text{m}$ at the localization of maxima near the frequencies 0.2, 0.28, and a very small maximum at 0.32 in the units of $[2\pi C/a]$. In between these peaks, the transmittance drops to 0%, therefore manifesting two band gaps with the resonant mode in the middle. Analysing the results in Fig. 2, it can be noticed that with increasing defect size the resonant mode frequency increases. The detailed behaviour of those peaks is visualized in Fig. 3. As can be seen, initially (black solid curve) at the smallest size of the defect, the frequency of the resonant mode changes only slightly towards higher frequencies, increasing it more rapidly above the defect size of 0.10 μm . Nevertheless, as the radius of the defect increases, the increase in frequency (or shift of the resonant mode toward higher frequencies) is maintained in the entire tested range. The transmittance coefficient for the resonance mode presents a much different relationship (see the blue dotted line in Fig. 3). Initially as the size of the defect increases, there is a small increase in transmittance, with a hardly noticeable increase between no defect and the smallest size considered ($r_d = 0.05 \mu\text{m}$). Then, when the defect radius exceeds 0.20 μm , the transmittance drops significantly to about 8% for $r_d = 0.25$ and 3% for $r_d = 0.30$. When there is no defect, so there is a normal $r_d = 0.36$ hole in the middle, the resonant mode vanishes completely.

In order to show the change between the periodic (PC) and hybrid structure presented in this article, we have computed the band structure of the waveguide in the case when periodicity of meta-atoms is conserved. For this reason, we constructed a cell with one hole ($r = 0.36 \mu\text{m}$) with PML's located on the top and bottom of the cell and periodic Bloch's conditions along the x direction. The resulting band structure is presented in Fig. 4.

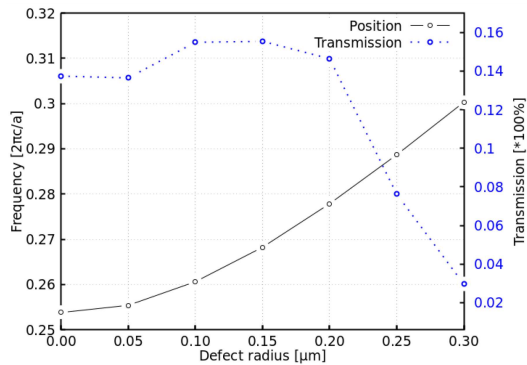


Fig. 3. Shift in resonant mode frequency and flux transmission for different defect sizes. Here the $r_d = 0.00 \mu\text{m}$ stands for “no hole” (lines connecting point for better visualization only).

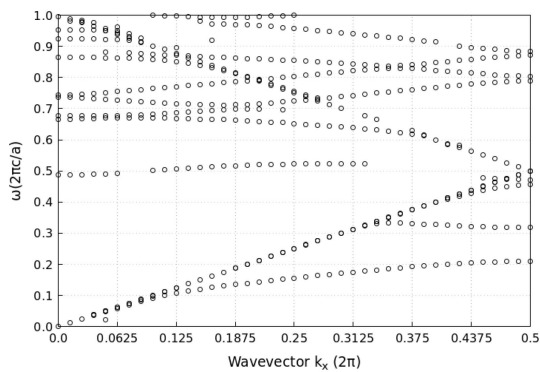


Fig. 4. Bandstructure diagram for perfect photonic crystal waveguide.

By analysing the band structure one can see that the perfect PC waveguide has bands that intersects in the entire frequency range, therefore it shows no resonant modes and no band gaps. This means that the emergence of the band gaps in the non-periodic waveguide is related to the defect itself, as can also be seen in Fig. 2 for the “no defect” curve (there is no resonance peak in between the frequencies ~ 0.2 and $\sim 0.32 [2\pi C/a]$).

4. Conclusions

In this paper, we have showed that by introducing a defect into the waveguide and modifying the size and type of this defect (hole or gap), the existence, position of the resonant peak, and the transmission of the resonant frequency electromagnetic wave associated with this mode can be manipulated, enabling so-called band gap engineering. The emergence of the band gaps is related to the presence of the defect and the trapping of the resonant mode inside this defect, which in turn is the effect of a finite number of surrounding holes. This in turn enables the resonant mode to leak into the waveguide and its surroundings. On the other hand, the resonance

mode could be used to transmit an electromagnetic wave with much greater efficiency if the wave source was precisely tuned to that frequency. The waveguide would be then considered as creating a narrow filter which may be useful to transmit signals for long range.

Acknowledgments

This research was supported in part by PLGrid Infrastructure.

References

- [1] S.P. Mohanty, S.K. Sahoo, A. Panda, G. Palai, *Optik* **185**, 146 (2019).
- [2] C.S. Mishra, A. Nayyar, S. Kumar, B. Mahapatra, G. Palai, *Optik* **176**, 56 (2019).
- [3] P. Jaturaphagorn, N. Chattham, P. Limsuwan, P. Chaisakul, *Results Opt.* **5**, 100174 (2021).
- [4] Qi Cheng, Shutao Wang, Jiangtao Lv, Junzhu Wang, Na Liu, *Opt. Commun.* **483**, 126640 (2021).
- [5] Y. Wu, Q. Liu, T. Liu, J. Wang, S. Xu, *J. Alloys Compd.* **911**, 164768 (2022).
- [6] F. Parandin, A. Sheykhan, *Opt. Laser Technol.* **151**, 108021 (2022).
- [7] A. Syouji, Y. Kamijyo, K. Fukushima, H. Ishihara, *J. Magn. Magn. Mater.* **551**, 168990 (2022).
- [8] L. Zhang, C. Zhu, S. Yu, Z. Zhou, D. Ge, *Results Phys.* **31**, 105054 (2021).
- [9] H.A. Gómez-Urrea, J. Bareño-Silva, F.J. Caro-Lopera, M.E. Mora-Ramos, *Photonic Nanostruct.* **42**, 100845 (2020).
- [10] D.M. Calvo-Velasco, R. Sánchez-Cano, *Curr. Appl. Phys.* **35**, 72 (2022).
- [11] A. Delitsyn, D.S. Grebenkov, *Appl. Math. Comput.* **412**, 126592 (2022).
- [12] R.C. Gauthier, S. Newman, K.E. Medri, *Opt. Commun.* **285**, 1976 (2012).
- [13] K. Saito, T. Tanabe, Y. Oyama, *Opt. Commun.* **365**, 164 (2016).
- [14] Y.-F. Wang, T.-T. Wang, J.-W. Liang, Y.-S. Wang, V. Laude, *J. Sound Vib.* **437**, 410 (2018).
- [15] Uwe Huebner, R. Boucher, W. Morgenroth, M. Schmidt, M. Eich, *Microelectron. Eng.* **83**, 1138 (2006).
- [16] S.S.M. Lis, K. Rajasimha, K. Debnath, V.K. Chaitanya, B.N. Shivakiran Bhaktha, *Opt. Mater.* **126**, 112114 (2022).
- [17] A.F. Oskooi, D. Roundy, M. Ibanescu, P. Bermel, J.D. Joannopoulos, S.G. Johnson, *Comput. Phys. Commun.* **181**, 687 (2010).